Available online at www.sciencedirect.com
SCIENCE DIRECT®
Journal of Photochemistry and Photobiology A: Chemistry 170 (2005) 7–14
Journal of Photochemistry and Photobiology A:Chemistry
www.elsevier.com/locate/jphotochem

Photocatalytic decolorization of methyl orange in aqueous medium of TiO_2 and Ag–TiO_2 immobilized on γ-Al_2O_3

Lung-Chuan Chen*, Fu-Ren Tsai, Chao-Ming Huang

Department of Environmental Engineering, Kun-Shan University of Technology, Yung Kang City, Tainan 710, Taiwan, ROC

Received 26 April 2004; received in revised form 5 July 2004; accepted 5 July 2004
Available online 25 August 2004

Abstract

TiO_2, synthesized through a sol–gel procedure with acetylacetone chelating agent, was immobilized on γ-Al_2O_3 and deposited with photoreduced Ag. The prepared catalysts were characterized and applied for decolorization of methyl orange (MO). The photoactivity of TiO_2/γ-Al_2O_3 is affected by the H_2O/Ti molar ratio applied in the sol–gel process. The optimal calcination temperatures of the TiO_2/γ-Al_2O_3 locate in the ranges from 723 to 773 K and 773 to 873 K as TiO_2 prepared with H_2O/Ti of 10 and 1, respectively. Incorporating photoreduced Ag to TiO_2/γ-Al_2O_3 leads to reduction reaction of methyl orange in addition to oxidation reaction, and yields a significant increment in decolorization efficiency. The optimal Ag load on TiO_2/γ-Al_2O_3 and dosage of Ag/TiO_2/γ-Al_2O_3 in the photodecolorization of methyl orange are about 1.0% and 1.0 g/L, respectively. The photocatalytic rate is proportional to the Ag load and catalyst dosage raised to the powers of 0.45 and 0.71, respectively.

Keywords: Photocatalytic; Methyl orange; Ag; TiO_2; γ-Al_2O_3

1. Introduction

Recently, photocatalytic processes have been receiving much attention, particularly for the complete destruction or mineralization of the toxic and non-biodegradable compounds to carbon dioxide and inorganic constituents in both water and gas phases [1–4]. Among the photocatalysts applied, titanium dioxide is the most popular one due to the peculiarities of chemical inertness, suitable bandgap energy, non-photocorrosion and non-toxic influence on the microorganisms, etc. Owing to the policies of efficient utilization of solar energy, high quantum efficiency and convenience of operation, the present researches of the photocatalytic processes have focused on the designs and constructions of new light energy sources, photochemical reactors, preparations of novel photocatalysts and their supports [1].

Irradiation of TiO_2 semiconductor by light with energy equal to or greater than its bandgap energy leads to excitation of an electron from the valence band to the conduction band. Charge separation is then formed. The electrons in the conduction band behave as a cathode and promote the reduction reactions of oxidized compounds with potentials positive to that of the lowest conduction band. On the other hand, positive holes (h^+) are generated in the valence band. The holes show high affinities for electrons and behave as an anode to oxidize the reduced compounds with potentials negative to that of the highest valence band or to oxidize the adsorbed H_2O or OH^- to hydroxyl radical ($HO^\bullet$). Hydroxyl radicals are very reactive neutral species, which react rapidly and non-selectively with the contaminants preadsorbed on titanium dioxide surface. Accordingly, $HO^\bullet$ is the chief oxidant for photocatalytic degradation in wastewater treatment [2,5].

In the past few years, titanium dioxide-suspended systems were widely applied for the photocatalytic processes. It revealed a fair photoactivity, but the separation of the finely powdered titanium dioxide from the slurry system was very difficult. Hence, the immobilization of TiO_2 on supports to improve the separated efficiency has attracted much attention.

* Corresponding author. Tel.: +886 6 2050137; fax: +886 6 2050540.
E-mail address: lcchen@mail.ksut.edu.tw (L.-C. Chen).

1010-6030/$ – see front matter © 2004 Elsevier B.V. All rights reserved.
doi:10.1016/j.jphotochem.2004.07.012

However, the immobilization usually decreases the overall photoactivity of TiO_2 [1,6–8]. Also, the blue shift of the absorption band occurs with immobilization, and then decreases the utilization of solar energy [9,10]. Recently, binary metal oxides systems, such as TiO_2/SiO_2 [11–15], were investigated to enhance photoactivity. An analysis of these systems reveals that large surface area and preferential adsorption of the reacted molecules on SiO_2 will promote the photoactivity [12]. Additionally, Fu et al. [11] indicated that the surface acidity of TiO_2 increased with addition of SiO_2. These surface acidic sites were said to be in the form of stronger surface hydroxyl groups, which accepted holes generated by illumination and sequentially oxidized the adsorbed molecules and prevented recombination of electrons and holes. Therefore, the photoactivity increases, however, it needs to be further improved for commercial application.

Aluminum oxide, with high surface area and acidity, is widely used as catalyst's support. Kato [16] also pointed out that γ-Al_2O_3 was not harmful to the photocatalytic activity of TiO_2. Furthermore, introduction of platinum or silver to the titanium dioxide photocatalytic system can increase the photocatalytic efficiency [2,17–21]. Unfortunately, few reports concerned about the immobilization of TiO_2 on γ-Al_2O_3 with deposited metal [13,21]. Accordingly, TiO_2/γ-Al_2O_3 photocatalysts with and without photodeposited Ag are prepared and characterized by X-ray diffraction (XRD), UV-diffusion reflectance spectroscopy and FTIR. Finally, methyl orange is used as a probe for the photocatalytic decolorization due to the relatively high toxicity and complex structure, which both make it difficult to be treated by microorganisms.

2. Experimental

γ-Al_2O_3 (Merck) with a surface area and a pore volume of 162 m^2/g and 0.45 cm^3/g, respectively, was used as carrier. The particle size of the γ-Al_2O_3 was sieved to be in the range from 200 to 270 mesh. Titanium isopropoxide (TTIP; TCI, EP), acetylacetone (ACAC; Lancaster, EP), ethanol (Scharlace, 99.8%), HCl (Ferak, GR) and silver nitrate (Katayama Chem. Co., special grade) were all used as received. Methyl orange (MO; Merck) was dissolved in ultra pure water (Milli Pore Q^+) to a desired concentration. The pH of the solution was adjusted to the desired value by NaOH or HCl and measured by a pH meter (Suntex, SP-701). The prepared MO solution was stored in the dark and used within a week.

A 0.5 M solution of TTIP in ethanol was prepared; subsequently, ACAC was added to result a clear-yellow solution. A molar ratio of ACAC/TTIP = 1 was used. The solution was stirred at room temperature for 3 h. H_2O of pH 1.5 or 7.0, adjusted by HCl and NaOH, was added drop by drop to the solution under vigorous stirring, and the prepared TiO_2 were designed as A- and N-types corresponding to the acidic and neutral media, respectively. The molar ratio of H_2O/TTIP was a studied factor and changed from 1 to 20. This sol was stirred at room temperature for 3 h, after which γ-Al_2O_3 powder was added slowly with vigorous stirring. The final solution was kept on stirring at 323 K for 24 h. The solid samples were filtered, washed by water and dried in air at 373 K for 24 h, eventually calcinated at the desired temperature for 3 h. Then, the TiO_2/γ-Al_2O_3 proceeded photoreduction [22] with silver nitration to make $Ag/TiO_2/\gamma$-Al_2O_3 photocatalysts by an UV light source (Philip, HPI–T400 W).

The bonding structures of the prepared photocatalysts were analyzed by FTIR (Jasco, FTIR-410 with DR-81). XRD (Rigaku D/Max III.V) technique and UV-diffusion reflection spectroscopy (Hitachi, U3010) were applied to study the crystal type and absorption bandgap energy. The surface area and pore volume were determined by BET method (Micromeritics, ASAP2400).

The photoactivity test was conducted in a Pyrex glass reactor of about 80 mm in diameter and 100 mm in height. The reactor was provided with a water jacket to control the reaction temperature. The cover of the reactor had ports for sampling, a thermal meter, a gas disperser and a condenser. A 400 W medium pressure mercury lamp (Philip, HPI-T400 W) was used as the light source. A magnetic stirrer operated at 600 rpm was used to provide a good mixing.

At the beginning of a run, 300 mL MO solution was fed to the reactor, and then it was kept at 303 K. The desired amount of the photocatalyst was added, and oxygen or nitrogen was bubbled through the gas disperser into the reactor at 250 mL/min. After 2 h premixing, to attain the adsorption equilibrium of MO on the photocatalyst, the run was started by illuminating the light source. Samples were periodically taken from the reactor and analyzed by an UV–vis spectrophotometer (Perkin-Elemer, λ2).

3. Results and discussion

3.1. Characteristics of the prepared TiO_2/γ-Al_2O_3 photocatalysts

Fig. 1 depicts the XRD profiles of the pure γ-Al_2O_3 carrier and $Ag/TiO_2/\gamma$-Al_2O_3 photocatalysts. It appears that the TiO_2 is amorphous after calcination at 473 K, and γ-Al_2O_3 surface is almost covered by TiO_2, since the peaks near 38° and 46° belong to γ-Al_2O_3 and are severely suppressed. Increasing calcination temperature to 673 K transfers TiO_2/γ-Al_2O_3 to the anatase phase. Further increasing the calcination temperature to 973 K yields the rutile phase in addition to the anatase phase. The fraction of rutile phase increases with decreasing H_2O/Ti applied in the sol–gel procedure. Incorporation of Ag to TiO_2/γ-Al_2O_3 cannot alter the XRD patterns and reveals no Ag diffraction peak, which may be ascribed to little content. The crystal size of TiO_2/γ-Al_2O_3 increases from 15.7 to 25.2, 10.5 to 20.1 and 8.5 to 17.7 nm as the calcination temperature increases from 673 to 973 K with H_2O/Ti of 1, 10 and 20, respectively, as shown in Fig. 2. With lower H_2O/Ti ratio, TTIP is not completely hydrolyzed and leads to larger crystal size. Also, increasing calcination

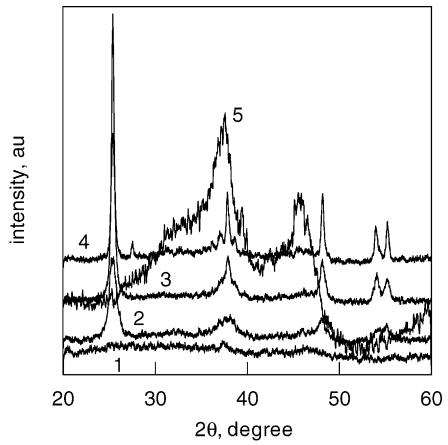

Fig. 1. The X-ray diffraction profiles of γ-Al_2O_3 and Ag/TiO_2/γ-Al_2O_3 with calcination temperature. Line 1: Ag (0.67%)/TiO_2/γ-Al_2O_3 calcinated at 473 K for 3 h; line 2: Ag (0.67%)/TiO_2/γ-Al_2O_3 calcinated at 673 K for 3 h; line 3: Ag (0.67%)/TiO_2/γ-Al_2O_3 calcinated at 873 K for 3 h; line 4: Ag (0.67%)/TiO_2/γ-Al_2O_3 calcinated at 973 K for 3 h; line 5: γ-Al_2O_3 calcinated at 473 K for 3 h.

temperature increases the dehydration between the adjacent Ti–OH groups and increases the crystal size.

Fig. 3 shows the UV-diffusion reflectance spectra of the samples calcinated at 873 K. Increasing TiO_2 content on TiO_2/γ-Al_2O_3 from 5 to 20 wt.% shifts the absorption band edge from 380 to 396 nm. However, further increasing the TiO_2 content to 30 wt.% cannot shift the absorption band edge to the longer wavelength. The results suggest that the blue shift occurred due to the quantization effect for the samples of low TiO_2 content. Incorporating Ag onto the TiO_2/γ-Al_2O_3 increases the absorption intensity, particularly in the visible region. Fig. 4 shows the absorption intensities of TiO_2 (30%)/γ-Al_2O_3 at 300 and 365 nm with H_2O/Ti ratio and calcination temperature. The 365 nm absorption intensity of TiO_2 (30%)/γ-Al_2O_3 decreases with increasing H_2O/Ti ratio, which may be ascribed to the influences of energy bandgap and blue shift effect since the crystal size decreases with increasing H_2O/Ti and decreasing calcination temperature.

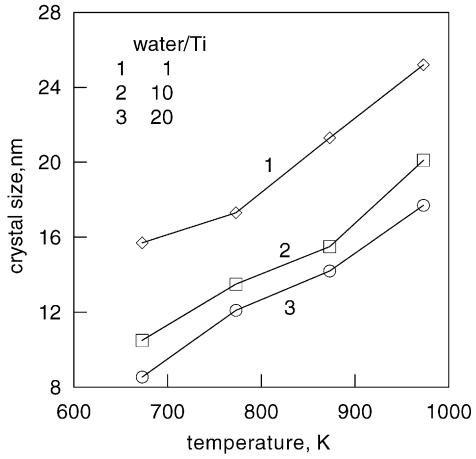

Fig. 2. Crystal size of A-TiO_2/γ-Al_2O_3 with calcination temperature.

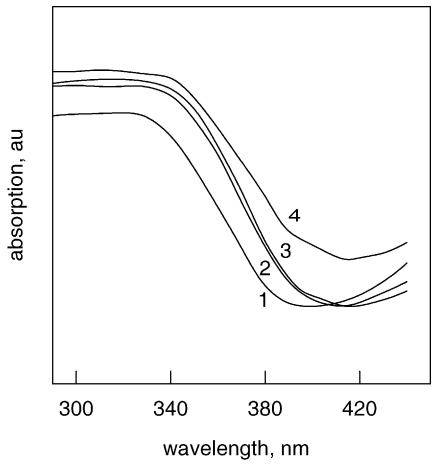

Fig. 3. The UV-diffusion reflectance spectra of Ag/A-TiO_2/γ-Al_2O_3 calcinated at 873 K. Line 1: TiO_2 (5%)/γ-Al_2O_3; line 2: TiO_2 (20%)/γ-Al_2O_3; line 3: TiO_2 (30%)/γ-Al_2O_3; line 4: Ag (0.67%)/TiO_2 (30%)/γ-Al_2O_3.

Lettmann et al. [23] reported that the carbon residues remained in TiO_2 after calcination, below 673 K, can absorb visible light. It is suspected that carbon residues existed in our samples after calcination below 773 K and affects the absorption intensity since the samples reveal a light-gray color, particularly for those with low H_2O/Ti. Increasing calcination temperature increases crystal size and decreases surface area, but it insignificantly affects the 365 nm absorption intensity since the inner surface of the samples contribute little to the absorption of irradiation. On the other hand, the 673 K-calcinated TiO_2/γ-Al_2O_3 with H_2O/Ti of 1 explores the least absorption intensity at 365 nm, which may be explained by incomplete crystallization owing to lower calcination temperature. The samples prepared with H_2O/Ti of 1 show the least 300 nm absorption intensity compared with those with H_2O/Ti of 10 and 20 since the influences of the blue shift and energy bandgap are absent at this wavelength. A significant decrease in 300 nm absorption intensity for the

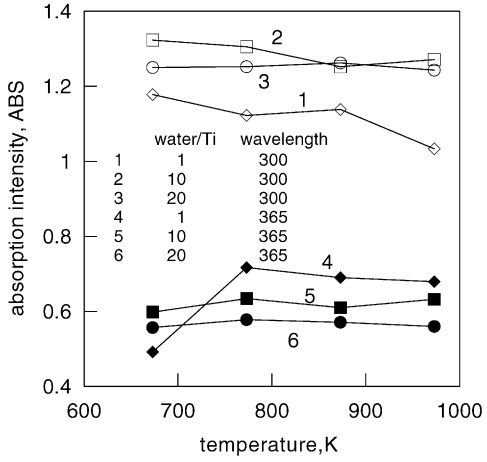

Fig. 4. Effect of calcination temperature on the absorption intensity of A-TiO_2/γ-Al_2O_3.

973 K-calcinated sample with H_2O/Ti of 1 is observed, possibly resulted from the effect of rutile phase, since it contains more rutile phase than those with H_2O/Ti of 10 and 20.

3.2. Photocatalytic decolorization of MO by TiO_2/γ-Al_2O_3

When the ratio of H_2O/Ti increases from 1 to 20, the photocatalytic rate of MO significantly increases from 0.05 to 0.25 μM/min and 0.03 to 0.25 μM/min using A- and N-TiO_2/γ-Al_2O_3 as catalysts, respectively, as shown in Fig. 5. When the ratio equals 1, TTIP is not properly hydrolyzed and TiO_2/γ-Al_2O_3 contains many organic residues and few Ti–OH groups. Hence, it needs higher temperature to remove the organic residues, however, a small surface area is then developed with temperature. Therefore, generation of electron–hole pair is suppressed. Also, the generated holes may have difficulties in separation and diffusion to the surface to react with the chemical species due to large dimension and organic residuals. Accordingly, the photocatalytic activity is low with low H_2O/Ti ratio. Increasing the H_2O/Ti ratio increases the hydrolysis level and then increases the Ti–OH groups. Hence, the nuclei number increases and the particle size decreases with H_2O/Ti ratio. A low calcination temperature is required to remove the organic residues. Consequentially, the surface area and the crystal size of TiO_2/γ-Al_2O_3 get large and small, respectively, and it reveals a better photocatalytic activity. When the H_2O/Ti ratio exceeds 10, water shows little influence on the photocatalytic activity since the hydrolysis extent of TTIP is not changed markedly with H_2O/Ti. Similar results were reported by Kato [16]. The results also suggest that the photocatalytic activity of the TiO_2/γ-Al_2O_3 prepared in the acidic solution is superior to that prepared in the neutral solution at lower H_2O/Ti ratio, and it may be ascribed to the acceleration of hydrolysis of TTIP by acid. However, this discrepancy disappears in the region of high H_2O/Ti.

Fig. 6 indicates that increasing the calcination temperature from 673 to 723 K increases the photocatalytic rates from 0.25 to 0.29 μM/min and 0.24 to 0.28 μM/min using A- and N-TiO_2/γ-Al_2O_3, prepared with H_2O/Ti ratio of 10. However, calcination with temperature exceeding 723 K significantly lowers the photocatalytic rate. On the other hand, TiO_2/γ-Al_2O_3 with H_2O/Ti of 1 reveals very low photoactivity as also shown in Fig. 6. The difference in the photocatalytic activity between A- and N-TiO_2/γ-Al_2O_3 catalysts with H_2O/Ti of 10 is insignificant since the influence of acid on the hydrolysis of TTIP is of little importance in the presence of acetylacetone chelating agent. When the calcination temperature increases to 723 K, the anatase phase develops near completely and the amount of Ti–OH group may remain at high level, therefore, an optimal photocatalytic rate is accomplished. However, calcination with higher temperature may change the surface states and significantly decrease the Ti–OH groups, which are mainly involved in the generation of hydroxyl radicals. Hence, the photocatalytic rate decreases with calcination temperature. Furthermore, when the calcination temperature increases to 973 K, the rutile phase of TiO_2 develops and leads to the significant decrease in photocatalytic rate.

Fig. 7 shows that increasing the calcination temperature from 673 to 973 K decreases the surface areas and MO adsorption amount of A-TiO_2/γ-Al_2O_3 with H_2O/Ti of 10 from 147 to 82 m^2/g and 2.62 to 1.48 μmol/g, respectively. The measured surface areas are all smaller than that of pure γ-Al_2O_3, which may be resulted from pore-blocking and surface-coverage of γ-Al_2O_3 by TiO_2 as well as existence of pure TiO_2 in addition to TiO_2/γ-Al_2O_3.

Decreasing pH from 10.6 to 4.5 increases the photocatalytic rate and equilibrium adsorption amount of MO

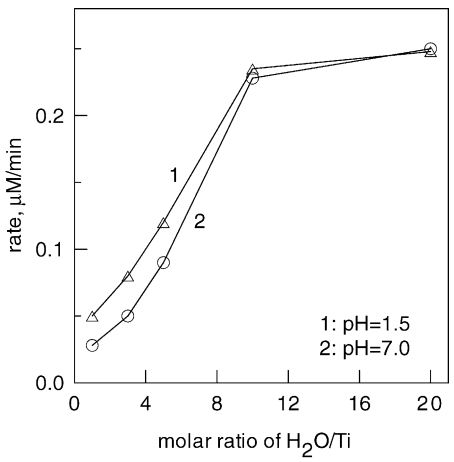

Fig. 5. Effect of H_2O/Ti molar ratio on the photocatalytic rate of MO. Catalyst: TiO_2 (30%)/γ-Al_2O_3; dosage: 1 g/L; calcination temperature: 773 K; initial MO concentration: 30.5 μM; oxygen flow rate: 250 mL/min; initial pH: 6.5; volume of solution: 300 mL; stir rate: 600 rpm; reaction temperature: 303 K.

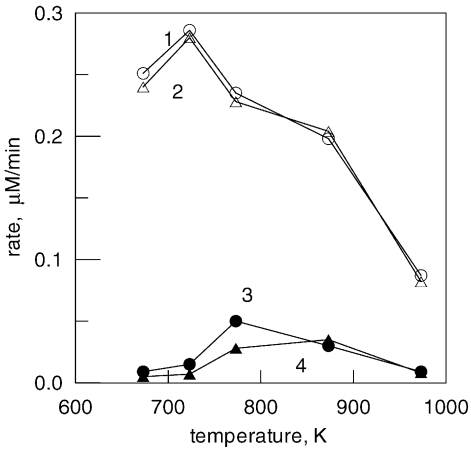

Fig. 6. Effect of calcination temperature on the photocatalytic rate of MO. Catalyst: TiO_2 (30%)/γ-Al_2O_3; dosage: 1 g/L; reaction temperature: 303 K; initial MO concentration: 30.5 μM; oxygen flow rate: 250 mL/min; initial pH: 6.5; volume of solution: 300 mL. Line 1: A-TiO_2, H_2O/Ti = 10; line 2: N-TiO_2, H_2O/Ti = 10; line 3: A-TiO_2, H_2O/Ti = 1; line 4: N-TiO_2, H_2O/Ti = 1.

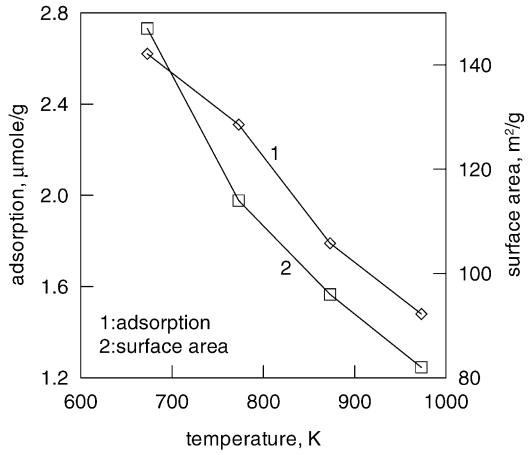

Fig. 7. Effect of calcination temperature on the surface area and MO adsorption of A-TiO_2 (30%)/γ-Al_2O_3. Initial MO concentration: 30.5 μM; adsorption temperature: 303 K; calcination temperature: 773 K; catalyst dosage: 1 g/L; initial pH: 4.5; volume of solution: 300 mL.

on TiO_2/γ-Al_2O_3 from 0.10 to 0.42 μM/min and 0.40 to 2.31 μmol/g, respectively, as shown in Fig. 8. Further decreasing pH to 3.0 dramatically increases the equilibrium adsorption amount to 9.06 μmol/g. MO is an indicator in aqueous solution, whose structure remains in the basic and acidic forms as pH is above 4.5 and below 3.1, respectively. Therefore, the influences of pH on the photocatalytic reaction may be mainly resulted from the variation of TiO_2 surface with pH in the range from 10.6 to 4.5. Crittenden et al. [2] indicated the photocatalytic activity of TiO_2 depended on the raw materials and methods applied to prepare the TiO_2. The surface of TiO_2 is abounded with Ti–OH groups, acidic bridged-hydroxyl groups, Ti–O–Ti linkages, water adsorbed on the Lewis acidic site and so on. Decreasing pH of MO solution increases the proton concentration and Ti–O–Ti linkages may react with protons to become the acidic bridged-hydroxyl and even to Ti–OH groups. These groups may be beneficial to generate the electron–hole pair. Additionally, decreasing pH increases the surface acidity of the catalyst, and then increases the adsorption amount of MO, especially below the point of zero charge (pH_{pzc}). Accordingly, the photocatalytic rate increases with decreasing pH. When pH decreases below 3.1, the structure of MO changes to the acid type and a tautomeric equilibrium occurs between the two acidic forms, which may be favorable to the adsorption in addition to the effects of surface acidity.

Increasing TiO_2 weight fraction on TiO_2/γ-Al_2O_3 from 2.5 to 40 wt.% increases photocatalytic rate and conversion of MO at 60 min from 0.11 to 0.44 μM/min and 15 to 65%, respectively, as shown in Fig. 9. The results also indicate that the increments in both rate and conversion become insignificant in the region of high TiO_2 content. A blue shift of the absorption band edge is expected if the TiO_2 content is too low, thereby affecting the threshold wavelength to generate electron–hole pairs. Additionally, low TiO_2 content may make an incomplete absorption of the incident photons. Accordingly, a poor photocatalytic rate is accomplished. On the other hand, a good dispersion of TiO_2 on γ-Al_2O_3 is expected in the region of low TiO_2 content. The acid property of the γ-Al_2O_3 may be advantageous to increase the surface acidity of TiO_2 and promote the photocatalytic rate. The effective enhancement in the surface concentration of MO on γ-Al_2O_3 neighboring to the TiO_2 site may also promote efficient decolorization by photogenerated species. Furthermore, increasing TiO_2 content increases the diffusion lengths of the photogenerated electrons and holes to the TiO_2 surface where the decolorization of MO occurs. Additionally, the shielding effect by the exterior TiO_2 may suppress the utilization of the interior TiO_2 and contribute little to the photocatalytic rate. Hence, the ratio of number of MO molecules decolorized to the number of the incident photons based on gram of TiO_2

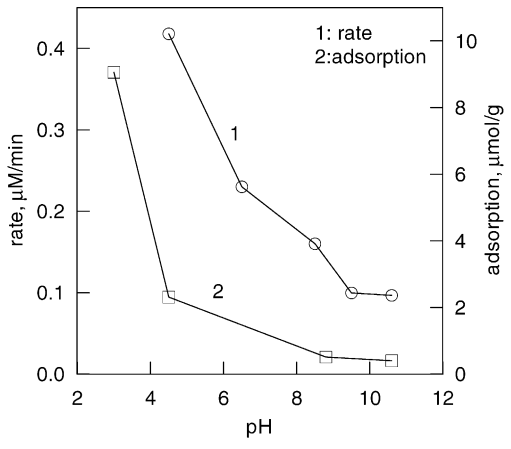

Fig. 8. Effect of initial pH of MO solution on the photocatalytic rate and adsorption of MO. Catalyst: A-TiO_2 (30%)/γ-Al_2O_3; dosage: 1 g/L; calcination temperature: 773 K; volume of solution: 300mL; initial MO concentration: 30.5 μM; oxygen flow rate: 250 mL/min; reaction temperature: 303 K.

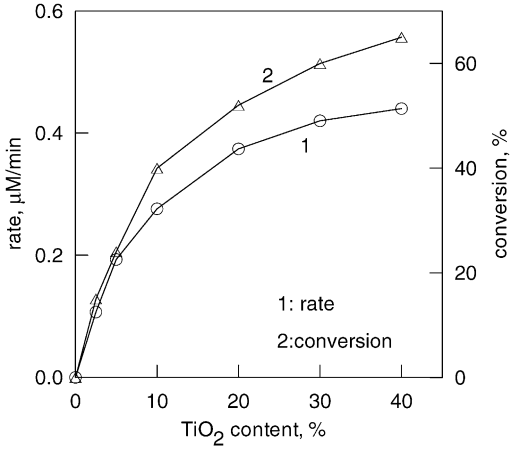

Fig. 9. Effect of TiO_2 content of A-TiO_2/γ-Al_2O_3 catalyst on the photocatalytic rate and conversion of MO. Volume of solution: 300 mL; initial MO concentration: 30.5 μM; oxygen flow rate: 250 mL/min; reaction temperature: 303 K; initial pH: 4.5, run time for conversion measured: 60 min; catalyst dosage: 1 g/L; calcination temperature: 773 K.

loaded on γ-Al_2O_3 decreases from 23.5 to 6.4% as the TiO_2 content increases from 2.5 to 40%. The optimal content of TiO_2 in the binary metal oxides depends on the kind of the second metal oxide, the prepared method, the photocatalytic reaction system and so on. Fu et al. [11] reported that the optimal TiO_2/SiO_2 and TiO_2/ZrO_2 weight ratios were 84/16 and 88/12, respectively, for the photodestruction of ethylene. While, Anderson and Bard [12] suggested that the TiO_2/SiO_2 ratio of 30/70 was the most effective for the photodecomposition of rhodanine-6G.

3.3. Enhancement of photocatalytic decolorization by Ag

The photocatalytic rate increases from 0.65 to 1.90 μM/min as the weight percentage of Ag on TiO_2 (30%)/γ-Al_2O_3 increases from 0.067 to 1.0 wt.%, further increasing the weight percentage of Ag to 1.23%, however, decreases the photocatalytic rate to 1.85 μM/min as shown in Fig. 10. The photogenerated electrons can be quickly transferred from TiO_2 to Ag, where they react with oxidized compounds. Therefore, Ag on TiO_2 can reduce the frequency of recombination of electrons and holes and enhance the photocatalytic rate. However, too much Ag on TiO_2 will interfere with the absorption of the incident illumination by TiO_2, furthermore, it may become a recombination center by introducing a new energy level between the valence band and the conduction band. Both decrease the photocatalytic rate.

A logarithm plot of the photocatalytic rate against the weight percentage of Ag on TiO_2 (30%)/γ-Al_2O_3 in the range from 0.067 to 0.67% yields a straight line with $R^2 = 0.97$ as also shown in Fig. 10. The slope is 0.45, indicating the photocatalytic rate is proportional to Ag load raised to the power of 0.45.

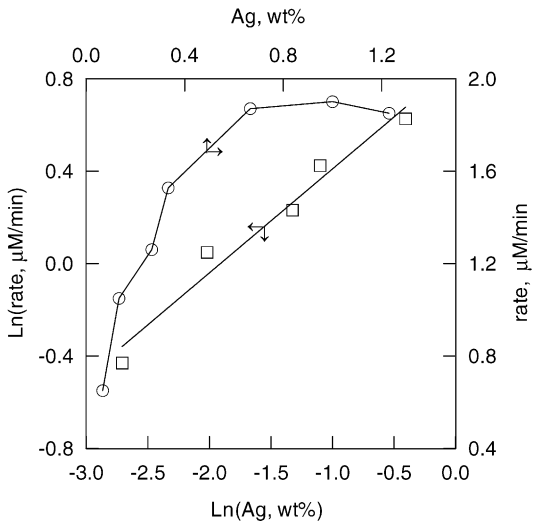

Fig. 10. Effect of Ag weight fraction of Ag/A-TiO_2/γ-Al_2O_3 on the photocatalytic rate of MO. Catalyst dosage: 1 g/L; calcination temperature: 773 K; initial pH: 4.5; volume of solution: 300 mL; initial MO concentration: 30.5 μM; oxygen flow rate: 250 mL/min; reaction temperature: 303 K.

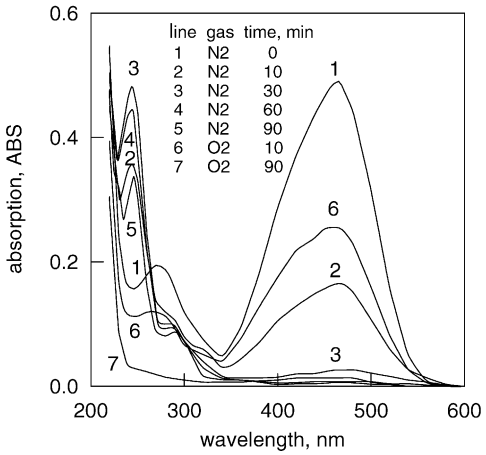

Fig. 11. The UV–vis spectra during the photocatalytic decolorization of MO. Catalyst: Ag (0.67%)/TiO_2 (30%)/γ-Al_2O_3; calcination temperature: 773 K; gas flow rate: 250 mL/min; reaction temperature: 303 K; initial pH: 4.5; volume of solution: 300 mL; initial MO concentration: 19.6 μM.

Fig. 11 shows the absorption changes of MO during the photocatalytic decolorization bubbling with nitrogen and oxygen using Ag (0.67%)/TiO_2 (30%)/γ-Al_2O_3 as catalyst. It indicates that photocatalytic decolorization rate of MO bubbling with nitrogen is superior to that with oxygen according to the main absorption peak at 465 nm. However, the absorption peak near 250 nm increases initially and then decreases when bubbling with nitrogen, but all the absorption peaks in the region of 200–600 nm monotonously decreases with run time when bubbling with oxygen. In the aerobic case, electrons on Ag react with adsorbed oxygen to form oxygen anion radicals ($O_2^{\bullet -}$), followed by a series reaction to become hydrogen peroxide and hydroxyl radical ($^{\bullet}OH$), promoting the photo-oxidation of MO. On the other hand, in the anaerobic case, electrons on Ag reduce MO, therefore, decolorization rate is elevated owing to the reduction process in addition to the oxidation one. The hydrazine is suspected to be one of the intermediates responsible for the increment of 250 nm absorption peak [24].

Increasing the Ag (0.67%)/TiO_2 (30%)/γ-Al_2O_3 dosage from 0.1 to 1.5 g/L increases the decolorization rate from 0.37 to 2.15 μM/min as shown in Fig. 12. It shows that the photocatalytic rate quickly increases with the catalyst dosage, however, it becomes less significant as the dosage further increases. The optimal dosage of catalyst may be affected by some factors, such as the volume of the reaction solution, reactor configuration, stir rate, intensity of the incident illumination and concentrations of reactants, etc. Suri et al. [17] studied the photocatalytic destruction of methyl–ethyl ketone (MEK), toluene and trichloroethylene, and reported that the optimal catalyst dosages were 0.1 and 1.0 g/L at the initial concentrations of 0.1 and 1.0–10 ppm, respectively. Ku and Hsieh [4] indicated that the optimal TiO_2 dosage for the photodestruction of 2,4-dichlorophenol was 1.4 g/L at the initial concentration of 3×10^{-4} M. A dosage of 1.0 g/L of Degussa P-25, providing the best results of the photooxidation

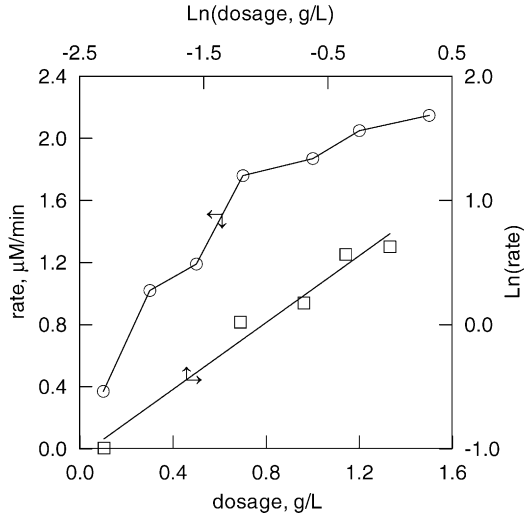

Fig. 12. Effect of $Ag/TiO_2/\gamma\text{-}Al_2O_3$ dosage on the photocatalytic rate of MO. Catalyst: Ag (0.67%)/TiO_2 (30%)/$\gamma\text{-}Al_2O_3$; calcination temperature: 773 K; oxygen flow rate: 250 mL/min; reaction temperature: 303 K; initial pH: 4.5; volume of solution: 300 mL; initial MO concentration: 30.5 μM.

of benzoic acid, was reported by Matthews [25]. Additionally, Crittenden et al. [2] pointed out that the optimal catalyst dosages were 0.2 and 0.5 g/L for the light intensities of 528.8 and 743.3 mW/L, respectively, at the initial trichloroethylene concentration of 15 ppm. Increasing TiO_2 dosage increases both absorption amount of the incident photons and amount of the adsorbed reactant. Consequently, the photocatalytic rate increases significantly with catalyst dosage, especially in the region of low dosage. On the other hand, a saturated dosage for the maximum absorption of the incident photons is achieved at a given intensity of illumination. Over the saturated dosage, increasing catalyst dosage cannot further increase the photocatalytic activity, even causes the negative influence on the photocatalytic activity due to the shielding effect and scattering of the incident illumination by the catalyst. Accordingly, an optimal photocatalyst dosage is achieved at a specified reaction condition.

A logarithm plot of the photocatalytic rate against the dosage of the catalyst gives a straight line with $R^2 = 0.96$. The slope is 0.71, indicating that the photocatalytic rate is proportional to photocatalyst dosage raised to the power of 0.71. Okamoto et al. [26] and Wei and Wan [27] reported that the photocatalytic rates were proportional to catalyst dosages raised to the powers of 0.5 and 0.6, respectively, for the photooxidation of phenol. Additionally, Kawaguchi and Furuya [28] demonstrated a proportional relationship between the destruction rate and TiO_2 dosage for the photodegradation of monochlorobenzene in aqueous titanium dioxide suspension. Truchi and Ollis [5] also pointed out that the relationship between the photocatalytic rate and the dosage of catalyst was complicated and related to surface states of TiO_2 and adsorption behaviors of the reactants and hydroxyl radicals, etc. Hence, the power of 0.71 obtained in this work seems reasonable when compared with other systems.

4. Conclusions

Variables of H_2O/Ti ratio, pH and calcination temperature relate to the hydrolysis of titanium isopropoxide and the surface states of TiO_2, and affect the photocatalytic rate. Protons can accelerate the hydrolysis of titanium isopropoxide and affect the photocatalytic activity for samples with low H_2O/Ti ratio, however, this effect gradually disappears with increasing H_2O/Ti ratio. Calcination can change Ti–OR into Ti–OH, however, the dehydration reaction is also accelerated with temperature. Hence, an optimal calcination temperature is achieved with H_2O/Ti ratio. Decreasing pH will change the surface state and surface acidity of the catalyst and increase MO adsorption, which is beneficial to photocatalytic rate. Incorporating of Ag on $TiO_2/\gamma\text{-}Al_2O_3$ significantly increases the photodecolorization rate. The photodecolorization rate in the anaerobic condition is superior to that in the aerobic condition due to the reduction of MO in addition to oxidation process using $Ag/TiO_2/\gamma\text{-}Al_2O_3$ as catalyst, however, the former shows poor mineralization efficiency.

Acknowledgments

The support of the National Science Council of ROC (NSC89-2211-E168-001) and Kun Shan University of Technology is gratefully acknowledged.

References

[1] A. Haarstrick, O.M. Kut, E. Heinzle, Environ. Sci. Technol. 30 (1996) 817–824.
[2] J.C. Crittenden, J. Liu, D.W. Hand, D.L. Perram, Water Res. 31 (1997) 429–438.
[3] S.E. Park, H. Joo, J.W. Kand, Sol. Energy Mater. Sol. Cells 80 (2003) 73–84.
[4] Y. Ku, C.B. Hsieh, Water Res. 26 (1992) 1451–1456.
[5] C.S. Truchi, D.F. Ollis, J. Catal. 122 (1990) 178–192.
[6] K. Tennakone, C.T.K. Tilakaratne, I.R.M. Kottegoda, Water Res. 31 (1997) 1909–1912.
[7] A. Fernandez, G. Lassaletta, V.M. Jimenez, A. Justo, A.R. Gonzalez-Elipe, J.-M. Herrmann, H. Tahiri, Y. Ait-Ichou, Appl. Catal. B: Environ. 7 (1995) 49–63.
[8] M. Anpo, N. Aikawa, Y. Kubokawa, M. Che, C. Louis, E. Giamello, J. Phys. Chem. 89 (1985) 5017–5021.
[9] Z. Liu, R.J. Davis, J. Phys. Chem. 98 (1994) 1253–1261.
[10] W. Choi, A. Termin, M.R. Hoffmann, J. Phys. Chem. 98 (1994) 13669–13679.
[11] X. Fu, L.A. Clark, Q. Yang, M.A. Anderson, Environ. Sci. Technol. 30 (1996) 647–653.
[12] C. Anderson, A.J. Bard, J. Phys. Chem. 99 (1995) 9882–9885.
[13] K. Domen, Y. Sakata, A. Kudo, K.I. Maruya, T. Onishi, Bull. Chem. Soc. Jpn. 61 (1988) 359–362.
[14] C. Anderson, A.J. Bard, J. Phys. Chem. B 101 (1997) 2611–2616.
[15] M.S. Vohra, K. Tanaka, Water Res. 37 (2003) 3992–3996.
[16] K. Kato, J. Ceram. Soc. Jpn. 101 (1993) 240–249.
[17] R.P.S. Suri, J. Liu, D.W. Hand, J.C. Crittenden, D.L. Perram, M.E. Mullines, Water Environ. Res. 65 (1993) 665–673.
[18] A. Dobosz, A. Sobczynski, Water Res. 37 (2003) 1489–1496.
[19] S. Kim, W. Choi, J. Phys. Chem. B 106 (2002) 13311–13317.

[20] W. Zhao, C. Chen, X. Li, J. Zhao, H. Hidaka, N. Serpone, J. Phys. Chem. B 106 (2002) 5022–5028.
[21] J.M. Herrmann, H. Tahiri, Y. Ait-Ichou, G. Lassaletta, A.R. Gonzalez-Elipe, A. Fernandez, Appl. Catal. B: Environ. 13 (1997) 219–228.
[22] B. Kraeutler, A.J. Bard, J. Am. Chem. Soc. 100 (1978) 4317–4318.
[23] C. Lettmann, K. Hildenbrand, H. Kisch, W. Macyk, W.F. Maier, Appl. Catal. B 32 (2001) 215–227.
[24] Y. Kim, M. Yoon, J. Mol. Catal. A: Chem. 168 (2001) 257–263.
[25] R.W. Matthews, Water Res. 24 (1990) 653–660.
[26] K.I. Okamoto, Y. Yamamoto, H. Tanaka, A. Itaya, Bull. Chem. Soc. Jpn. 58 (1985) 2023–2028.
[27] T.-Y. Wei, C.-C. Wan, Ind. Eng. Chem. Res. 30 (1991) 1293–1300.
[28] H. Kawaguchi, M. Furuya, Chemosphere 21 (1990) 1435–1440.